Carcinogenesis, 2016, Vol. 37, No. 11, 1041–1051

doi:10.1093/carcin/bgw093
Advance Access publication September 7, 2016
Original Manuscript

ORIGINAL MANUSCRIPT

TGF-β-induced stromal CYR61 promotes resistance to gemcitabine in pancreatic ductal adenocarcinoma through downregulation of the nucleoside transporters hENT1 and hCNT3

Rachel A.Hesler[1], Jennifer J.Huang[1], Mark D.Starr[2], Victoria M.Treboschi[2], Alyssa G.Bernanke[2], Andrew B.Nixon[2], Shannon J.McCall[3], Rebekah R.White[4] and Gerard C.Blobe[1,2,*]

[1]Department of Pharmacology and Cancer Biology, [2]Division of Medical Oncology, Department of Medicine, [3]Department of Pathology and [4]Department of Surgery, Duke University, B354 LSRC Research Drive, Box 91004, Durham, NC 27708, USA

*To whom correspondence should be addressed. Tel: +1 919 668 1352; Fax: +1 919 681 6906; Email: gerard.blobe@duke.edu

Abstract

Pancreatic ductal adenocarcinoma (PDAC) is a lethal cancer in part due to inherent resistance to chemotherapy, including the first-line drug gemcitabine. Although low expression of the nucleoside transporters hENT1 and hCNT3 that mediate cellular uptake of gemcitabine has been linked to gemcitabine resistance, the mechanisms regulating their expression in the PDAC tumor microenvironment are largely unknown. Here, we report that the matricellular protein cysteine-rich angiogenic inducer 61 (CYR61) negatively regulates the nucleoside transporters hENT1 and hCNT3. CRISPR/Cas9-mediated knockout of CYR61 increased expression of hENT1 and hCNT3, increased cellular uptake of gemcitabine and sensitized PDAC cells to gemcitabine-induced apoptosis. In PDAC patient samples, expression of *hENT1* and *hCNT3* negatively correlates with expression of *CYR61*. We demonstrate that stromal pancreatic stellate cells (PSCs) are a source of CYR61 within the PDAC tumor microenvironment. Transforming growth factor-β (TGF-β) induces the expression of CYR61 in PSCs through canonical TGF-β-ALK5-Smad2/3 signaling. Activation of TGF-β signaling or expression of CYR61 in PSCs promotes resistance to gemcitabine in PDAC cells in an *in vitro* co-culture assay. Our results identify CYR61 as a TGF-β-induced stromal-derived factor that regulates gemcitabine sensitivity in PDAC and suggest that targeting CYR61 may improve chemotherapy response in PDAC patients.

Introduction

PDAC is the fourth leading cause of cancer death in the United States, with more than 40000 patient deaths per year (1). Moreover, PDAC is projected to become the second leading cause of cancer death by 2030 due to a rising incidence and the lack of improvement in survival compared with other cancers (2). PDAC has one of the lowest 5-year survival rates at 6% (1), underscoring the need for better treatment options. Gemcitabine is a nucleoside pyrimidine analog that has long been the backbone of chemotherapy for PDAC, both as a single agent, and more recently, in combination with nab-paclitaxel. Gemcitabine is utilized in first- and second-line treatment for locally advanced and metastatic PDAC, as well as adjuvant therapy for these patients. Incorporation of gemcitabine into DNA results in masked-chain termination, which stops DNA synthesis and induces apoptosis of the cell (3). Although gemcitabine is one of the most commonly used treatments for PDAC, as a single agent it prolongs median survival by just over a month and is not effective for all patients (4). Attempts to enhance gemcitabine efficacy with

Received: March 10, 2016; **Revised:** August 9, 2016; **Accepted:** August 16, 2016

Abbreviations

α-SMA	α-smooth muscle actin
CA-ALK5	constitutively active ALK5
CYR61	cysteine-rich angiogenic inducer 61
dCK	deoxycytidine kinase
ECM	extracellular matrix
EMT	epithelial-to-mesenchymal transition
hCNT3	human concentrative nucleoside transporter-3
hENT1	human equilibrative nucleoside transporter-1
NBMPR	S-(4-Nitrobenzyl)-6-thioinosine
PDAC	pancreatic ductal adenocarcinoma
PDX	patient-derived xenograft
PSC	pancreatic stellate cells
TGF-β	transforming growth factor-β

targeted agents or other cytotoxic agents, with the exception of nab-paclitaxel, have had limited success (5).

Because gemcitabine is hydrophilic, it must be transported through the hydrophobic cell membrane by transmembrane nucleoside transporters. The equilibrative nucleoside transport family mediates bidirectional transport of nucleosides across the plasma membrane along the concentration gradient, whereas the concentrative nucleoside transport family concentrates nucleosides in the cell by coupling transport with cations (6,7). Human equilibrative nucleoside transporter-1 (hENT1) and human concentrative nucleoside transporter-3 (hCNT3) both have important roles in the cellular uptake of the nucleoside analog gemcitabine (8). Consistent with this role, PDAC patients with low expression of hENT1 and hCNT3 have significantly worse survival after gemcitabine treatment compared with patients with high hENT1 and hCNT3 expression (9–12). Although hENT1 expression is currently being evaluated as a biomarker to predict patient response to gemcitabine (13), the molecular mechanisms regulating hENT1 and hCNT3 expression in the PDAC tumor microenvironment are largely unknown. Recent studies suggest that epithelial-to-mesenchymal transition (EMT) (14) and ErbB2 expression (15) negatively regulate hENT1 and hCNT3 expression, but further studies are needed to identify mechanisms that regulate their expression in PDAC cells in the context of the tumor microenvironment. Here, we investigate factors regulating hENT1 and hCNT3 expression in the PDAC tumor microenvironment.

Methods and materials

Cell culture and reagents

PANC1, MiaPaCa-2, BxPC3, CFPAC-1 and 293T cells were obtained from American Type Culture Collection (Manassas, VA) and were verified by Short Tandem Repeat analysis. After verification, cells were cultured for <1 month before being frozen, and all experiments were performed with <6 months of culturing. L3.6p cells were provided by Dr Isaiah Fidler (MD Anderson) (16). RLT-PSC human pancreatic stellate cells (PSCs) were provided by Dr Ralf Jesenofsky (University of Heidelberg) (17); HPSC-T human PSCs were provided by Dr Rosa Hwang (MD Anderson) (18); LTC-14 rat PSCs were provided by Dr Gisele Sparman (University Hospital of Rostock) (19) and imPSC mouse PSCs were provided by Dr Raul Urrutia (Mayo Clinic) (20). Both human and murine PSCs were obtained directly from the labs that isolated the cells and were functionally validated by their expression patterns in the indicated studies. All cells were grown at 37°C at 5% CO_2. PANC1, L3.6p, LTC-14, HPSC-T, RLT-PSC and imPSC cells were grown in Dulbecco's Modified Eagle Medium (DMEM) with 1 mM sodium pyruvate and 10% fetal bovine serum (FBS). MiaPaCa-2 cells were grown in DMEM with 1 mM sodium pyruvate, 10% FBS and 2.5% horse serum. CFPAC-1 cells were grown in Iscove's Modified Dulbecco's Medium (IMDM) with 10% FBS. BxPC3 cells were grown in RPMI-1640 media containing 1 mM sodium pyruvate, 10 mM HEPES (4-(2-hydroxyethyl)-1-piperazineethanesulfonic acid) and 10% FBS. Conditioned media (CM) from cells was concentrated by centrifugation using an Amicon Ultra-15 cellulose filter with a molecular weight cutoff of 3 kDa from Millipore (Billerica, MA). Chemical inhibitors against ALK5 (SB431542), p38 MAPK (SB203580) and PI3K (LY294002) were purchased from Cell Signaling Technology (Danvers, MA) and dissolved in DMSO. TGF-β1 ligand was purchased from R&D Systems (Minneapolis, MN). Gemcitabine (2, 2- difluoro-2-deoxycytidine) was purchased from the Duke Hospital Pharmacy Store Room. The hENT1 inhibitor S-(4-Nitrobenzyl)-6-thioinosine (NBMPR) was purchased from Sigma-Aldrich (St Louis, MO) and dissolved in DMSO.

Adenovirus

HA-tagged constitutively active ALK5 adenovirus (HA-ALK5^{T204D}) was provided by Dr Carlos Arteaga (Vanderbilt University) (21). The luciferase control and mouse CYR61 adenoviruses were provided by Dr Brahim Chaqour (SUNY Downstate) (22,23). Adenoviruses were generated and purified using the Adeno-X Maxi Purification Kit from Clontech (Mountain View, CA). Adenovirus titer was determined using the Adeno-X Rapid Titer Kit from Clontech, and cells were infected at the indicated multiplicity of infection (MOI).

Lentivirus

Lentivirus CRISPR constructs targeting hCYR61, rSmad2 and rSmad3 were made using the LentiCRISPRv2 vector (Addgene Plasmid 52961) following the GeCKO protocol (24,25). Briefly, the lentiCRISPRv2 vector was digested by BsmB1 and de-phosphorylated by CIP alkaline phosphatase. sgRNA target sequences were designed using the GeCKO library (24,25) (sequences listed in Supplementary Table S1, available at *Carcinogenesis* Online), and the synthesized oligos were annealed and phosphorylated using T4 polynucleotide kinase. The annealed sgRNA target sequence oligos were ligated into the digested lentiCRISPRv2 backbone using T4 DNA ligase. The ligated DNA was transformed into One Shot Stabl3 competent cells and selected on LB-Amp plates. Each construct was sequenced to verify correct incorporation of the sgRNA target sequence into the lentiCRISPRv2 vector. To generate lentivirus for each lentiCRISPRv2 construct, a 10 cm dish of 293T cells was transfected with 4.5 μg of the respective lentiCRISPRv2 construct along with 2.25 μg PAX2, 0.75 μg pMD2.G and 18 μl Xtremegene. Media was changed on the 293T cells the morning after transfection. At 48 and 72 h later, the 293T media containing lentivirus was harvested and filtered through a 0.45 μm cellulose filter. The media was applied to MiaPaCa-2, PANC1 or LTC-14 cells with 6 μg/ml polybrene. Stably infected cells were selected using 2 μg/ml puromycin. Single cell clones were isolated for MiaPaCa-2 and PANC1 hCYR61 CRISPR to achieve knockout of expression. For rSmad2 and rSmad3, the CRISPR/Cas9 vectors were stably introduced, and the bulk populations of cells with partial knockdown were used.

Western blotting

Total cell lysates were harvested, boiled in sample buffer, separated by sodium dodecyl sulfate-polyacrylamide gel electrophoresis, transferred onto nitrocellulose membranes, blocked in 5% milk in Tris-buffered saline and incubated overnight with the primary antibody of interest in 5% bovine serum albumin (BSA) in Tris-buffered saline (TBS)/0.1% TWEEN. Quantification was performed

using the LICOR Odyssey (Lincoln, NE) software by taking the integrated intensity of each band and normalizing to the integrated intensity of the β-actin band. Antibodies against cleaved caspase 3 (9664), P-Smad2 (3101), Total Smad2 (3103), P-p38 MAPK (4511), Total p38 MAPK (9212), P-Akt (4058), Total Akt (4691) and Total Smad3 (9523) were all purchased from Cell Signaling Technology. Antibodies against human CYR61 (sc-13100) and hENT1 (sc-134501) were purchased from Santa Cruz Biotechnology (Dallas, TX). Antibodies against hCNT3 (HPA024729) and β-actin (A5441) were purchased from Sigma-Aldrich. Antibodies against rat/mouse CYR61 (ab24448) and fibronectin (ab2413) were purchased from Abcam (Cambridge, UK). The antibody for E-cadherin (610182) was purchased from BD Biosciences (San Jose, CA). Anti-rabbit IgG and anti-mouse IgG secondary antibodies were purchased from Cell Signaling (5470 and 5151) and LICOR (926-32212 and 926-32213).

Microarray and RNAseq dataset analysis

Patient mRNA microarray expression data were obtained from publically available datasets on NCBI Gene Expression Omnibus (GEO) for GDS4103 and GSE43288 (26,27). The GDS4103 platform was Affymetrix Human Genome U133 Plus 2.0 Array. The GSE43288 platform was Affymetrix Human Genome U133A Array (GPL96). All microarray data were $\log_2$ transformed. We queried the datasets using the gene probes listed in Supplementary Table 2, available at *Carcinogenesis* Online. Survival analysis of PDAC patients based on *CYR61* expression was obtained using publically available RNAseq data in the ICGC PACA-AU Data Portal (28). Patients were divided in half into high and low CYR61 expressing groups based on normalized read count of *CYR61* expression using Gene ID ENSG00000142871. For analysis of the cellular source of CYR61 within the tumor, *CYR61* mRNA expression in isolated PSCs, patient-derived xenografts, PDAC samples and tumor-derived PDAC cell lines was obtained from previously published RNAseq expression data (29).

hENT1 transport assay

[^{3}H]gemcitabine (16.32 µg/ml, 16.2 Ci/mmol) was purchased from Moravek Biochemicals (Brea, CA). Cells were incubated in transport buffer (20 mM Tris/HCl, 3 mM K_2HPO_4, 5 mM glucose, 130 mM NaCl, 1 mM $MgCl_2$-$6H_2O$ and 2 mM $CaCl_2$) as previously described (30). Cells were plated in 12 well plates at 150 000 cells/well (MiaPaCa-2) or 90 000 cells/well (PANC1). The following day, cells were rinsed in transport buffer then incubated with 100 nM [^{3}H]gemcitabine in transport buffer for 2 min (MiaPaCa-2) or 30 s (PANC1). When indicated, cells were pretreated for 10 min with doses of the hENT1 inhibitor NBMPR or DMSO control in transport buffer, and NBMPR or DMSO was included in 100 nM [^{3}H]gemcitabine incubation. After incubation, cells were rinsed three times with transport buffer containing 5 µM NBMPR to inhibit efflux of [^{3}H]gemcitabine. Cells were lysed in 1% (v/v) Triton-X-100, and protein concentration was determined using a bicinchoninic acid (BCA) assay from Thermo Scientific (Waltham, MA). Cell lysates were added to Ultima Gold from Perkin Elmer (Waltham, MA) and cell-associated radioactivity in counts per minute (CPM) was determined using a liquid scintillation counter. [^{3}H]Gemcitabine transport was calculated by normalizing CPM to protein concentration for each well. Each condition was performed in triplicate, and the experiment was repeated three times.

RT-PCR

RNA was extracted using the Quick-RNA™ MiniPrep kit from Zymo Research (Irvine, CA) according to kit instructions. Five hundred nanograms of RNA was reverse transcribed using the iScript cDNA Synthesis Kit from BioRad (Hercules, CA) following kit instructions. Each PCR reaction contained 1 µl of cDNA, 8 µl of H_2O, 10 µl of SYBRGreen Mix from BioRad and 0.5 µl each of respective forward and reverse primers. Primer sequences are listed in Supplementary Table 4, available at *Carcinogenesis* Online. PCR was performed as follows: 2 min at 94°C then 50 rounds at 94°C for 45 s, 56.8°C for 45 s, 72°C for 45 s, then 7 min at 72°C. The fold change in expression was determined by calculating $2^{(-\Delta\Delta C_T)}$, with glyceraldehyde 3-phosphate dehydrogenase (GAPDH) used as a reference gene. RT-PCR was performed in triplicate for each gene.

Titer glow cell viability assay

Cells were plated in 96 well opaque plates from Perkin Elmer and treated in triplicate for 48 h with indicated doses of gemcitabine. The viability of cells was measured using the CellTiter-Glo® Luminescent Cell Viability Assay from Promega (Madison, WI) and normalized to the untreated condition.

Immunohistochemistry

Immunohistochemical (IHC) staining for CYR61 was performed on paraffin-embedded tissue samples verified to be PDAC by a board-certified pathologist. PDAC tissues were de-paraffinized and re-hydrated, and antigen retrieval was performed in Target Retrieval Solution from Dako North America (Carpinteria, CA) in a 95°C water bath. Tissues were blocked with Peroxidazed 1 and Background Punisher from BioCare Medical (Concord, CA) before incubation with primary antibody for 2 h at room temperature. CYR61 antibody (Santa Cruz sc-13100) was diluted 1:25, and α-smooth muscle actin (α-SMA; Sigma-Aldrich 5228) diluted was 1:4000, both in Antibody Diluent from Dako North America. Tissues were washed in TBS with 0.1% Tween 20. Tissues were then treated with the HRP-Polymer Mach 4 detection system and Warp Red Chromagen from Biocare Medical following manufacturer's recommended protocol. Slides were counterstained with hematoxylin and Tacha's Bluing Solution from Biocare Medical. IHC was performed on tissue samples from nine PDAC patients. The study was conducted with approval of the Duke IRB, and informed consent was received.

CYR61 ELISA

The CYR61 ELISA kit was purchased from R&D Systems (DCYR10), and the ELISA was performed according to kit instructions. All patient serum samples were de-identified, and informed consent was received. The study was conducted with approval of the Duke IRB. Serum was obtained from 5 cc blood at the time of a diagnostic blood draw from subjects with confirmed PDAC.

In vitro co-culture assay

LTC-14 or imPSC pancreatic stellate cells were infected with adenovirus at indicated MOIs. After 24 h infection, PSCs were washed with phosphate-buffered saline, and media was replaced to start collecting CM. After 24 h, PSC CM was harvested and filtered through a 0.45 µM cellulose filter then applied to PDAC cells. After 24 h incubation, PSC CM was refreshed, and PDAC cells were then treated with gemcitabine for 48 h at indicated doses. Adherent and floating PDAC cells were collected for western blot analysis of cleaved caspase 3 levels.

Statistics

All statistical analyses were conducted with GraphPad Prism software. For all experiments, significance was set at $P < 0.05$. All *in vitro* experiments were analyzed using parametric statistics [two-sided *t* test or analysis of variance (ANOVA) with indicated *post hoc* test] and expressed as the mean ± SEM. Microarray expression

data and ELISA on serum samples were analyzed using nonparametric statistics (Mann–Whitney *U*, Wilcoxon matched pairs signed rank test or Kruskal–Wallis global test). Linear regression was performed on microarray data with the R^2 value, *P* value and slope for the line of best fit reported for each comparison. Survival curves were analyzed with log-rank statistics.

Results

CYR61 promotes chemoresistance by negatively regulating gemcitabine transport through hENT1 and hCNT3

To identify potential regulators of hENT1 and hCNT3 in the PDAC microenvironment, we analyzed a publically available microarray dataset of PDAC tumor samples (26) to identify genes whose expression significantly correlated with expression of *hENT1* (*SLC29A1*) and *hCNT3* (*SLC28A3*) and whose expression is significantly altered in PDAC tumor samples compared with normal adjacent tissue (Supplementary Figure 1A, available at *Carcinogenesis* Online). We identified 25 genes whose expression significantly correlated with both *hENT1* and *hCNT3* and whose expression is significantly altered in pancreatic cancer (Supplementary Table 3, available at *Carcinogenesis* Online). We were particularly interested in investigating cysteine-rich angiogenic inducer 61 (CYR61) because *CYR61* expression is increased in cancer and negatively correlates with *hENT1* and *hCNT3* expression. Additionally, CYR61 is a secreted matricellular protein that can be targeted using a neutralizing antibody, which indicates it has the potential to be targeted clinically. CYR61 is a member of the CCN family of matricellular proteins, which includes connective tissue growth factor (CTGF) and nephroblastoma overexpressed (NOV). The CCN family regulates diverse cell behaviors in a context-specific manner, primarily through interacting with integrins and heparin sulfate proteoglycans to activate downstream signaling (31).

The mRNA expression of *SLC29A1* (*hENT1*) and *SLC28A3* (*hCNT3*) negatively correlated with *CYR61* mRNA expression in PDAC patient samples (Figures 1A and B), indicating that CYR61 may play a role in suppressing expression of the nucleoside transporters that mediate cellular uptake of gemcitabine in the PDAC tumor microenvironment. *CYR61* expression did not significantly correlate with the expression of other nucleoside transporters in PDAC patient samples (Supplementary Figure 1B–F, available at *Carcinogenesis* Online), suggesting specific regulation of hENT1 and hCNT3. To examine whether CYR61 negatively regulated hENT1 and hCNT3 expression, we used CRISPR/Cas9 technology to knockout CYR61 expression in two PDAC cell lines with high CYR61 expression. We confirmed that CRISPR knockout decreased the soluble secreted CYR61 present in the CM (Supplementary Figure 2A and B, available at *Carcinogenesis* Online). CRISPR-mediated knockout

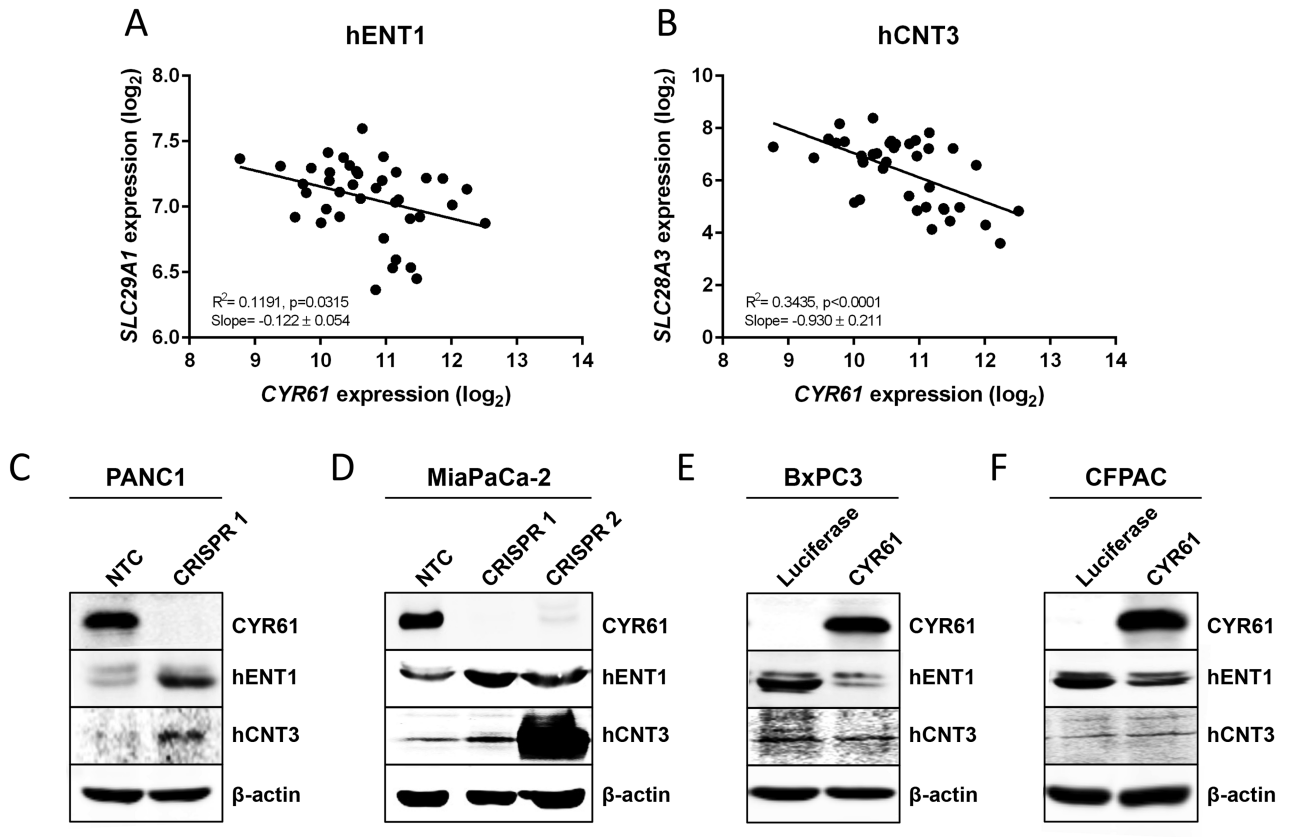

Figure 1. CYR61 negatively regulates the nucleoside transporters hENT1 and hCNT3 in PDAC cells. (**A**, **B**) Linear regression using the microarray dataset GDS4103. *n* = 39 patient samples: (**A**) *hENT1* (*SLC29A1*) and (**B**) *hCNT3* (*SLC28A3*). (**C**) Western blots for CYR61 (Santa Cruz), hENT1 and hCNT3 in PANC1 NTC and CYR61 CRISPR 1 knockout cells. Results are representative of five independent experiments. (**D**) Western blots for CYR61 (Santa Cruz), hENT1 and hCNT3 in MiaPaCa-2 cells for NTC, CYR61 CRISPR 1 and CYR61 CRISPR 2 knockout cells. Results are representative of four independent experiments. (**E**) Western blots for CYR61 (Abcam), hENT1 and hCNT3 in BxPC3 cells infected with CYR61 adenovirus or control luciferase adenovirus at an MOI of 100 for 48 h. Results are representative of three independent experiments. (**F**) Western blots for CYR61 (Abcam), hENT1 and hCNT3 in CFPAC cells infected with CYR61 adenovirus or control luciferase adenovirus at an MOI of 100 for 48 h. Results are representative of three independent experiments. (**B–F**) Western blotting results are quantified in Supplementary Figure 2.

of CYR61 significantly increased hENT1 and hCNT3 expression in PANC1 cells (Figure 1C; Supplementary Figure 2C, available at *Carcinogenesis* Online). Knockout of CYR61 also significantly increased hENT1 expression in MiaPaCa-2 cells, and increased hCNT3 expression, albeit with larger increases in CRISPR 2 cells (Figure 1D, Supplementary Figure 2D, available at *Carcinogenesis* Online). In a reciprocal manner, adenovirus-mediated overexpression of CYR61 in BxPC3 and CFPAC cells, which have low basal CYR61 expression, significantly decreased hENT1 expression (Figure 1E and F, Supplementary Figure 2E and F, available at *Carcinogenesis* Online). All cell lines had low basal expression of hCNT3 as previously reported for *in vitro* cell culture conditions (14), so overexpression of CYR61 in BxPC3 and CFPAC cells was not able to further decrease these low basal levels of hCNT3 expression. In PANC1 cells, treatment with gemcitabine for 48 h induced downregulation of hENT1, with knockout of CYR61 increasing hENT1 levels and blunting the effects of gemcitabine-mediated downregulation (Supplementary Figure 2G, available at *Carcinogenesis* Online).

To determine whether the CYR61 knockout-mediated increases in hENT1 and hCNT3 in PDAC cells resulted in higher cellular uptake of gemcitabine, we performed gemcitabine transport assays using radiolabeled ^{3}H-gemcitabine as previously described (30). Increasing doses of the hENT1 specific inhibitor NBMPR dramatically decreased the levels of ^{3}H-gemcitabine transported into the cell, showing specificity of the assay and supporting hENT1 as the major gemcitabine transporter in MiaPaCa-2 and PANC1 cells (Figure 2A). CRISPR-mediated knockout of CYR61 significantly increased the amount of ^{3}H-gemcitabine transported into PANC1 (Figure 2B) and MiaPaCa-2 cells (Figure 2C). These data indicate that the upregulation of hENT1 and hCNT3 following CRISPR knockout of CYR61 results in enhanced cellular uptake of gemcitabine.

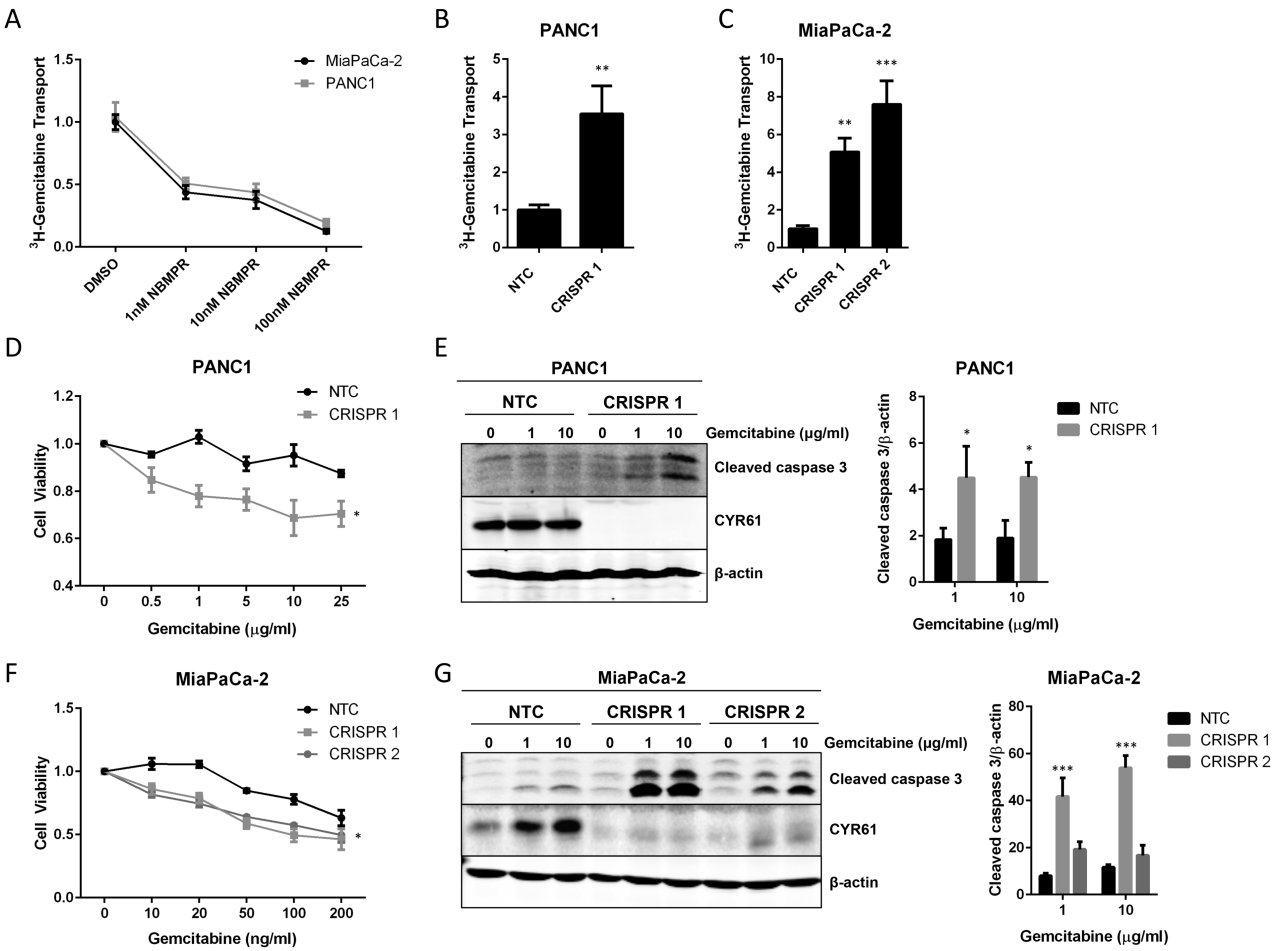

Figure 2. CYR61 inhibits gemcitabine transport and promotes resistance to gemcitabine-induced apoptosis. (**A**) Gemcitabine transport assay in MiaPaCa-2 and PANC1 cells using hENT1 inhibitor NBMPR at indicated doses. Gemcitabine transport expressed as CPM/protein normalized to DMSO. $n = 3$ independent replicates, each condition performed in triplicate. (**B**) Gemcitabine transport assay in PANC1 cells. Gemcitabine transport expressed as CPM/protein normalized to NTC. *t* test $^{**}P = 0.0039$. $n = 3$ independent replicates, each condition performed in triplicate. (**C**) Gemcitabine transport assay in MiaPaCa-2 cells. Gemcitabine transport expressed as CPM/protein normalized to NTC. ANOVA/Fisher's LSD, NTC versus CR1 $^{**}P = 0.0023$, NTC versus CR2 $^{***}P < 0.0001$. $n = 3$ independent replicates, each condition performed in triplicate. (**D**) Cell Titer Glo assay measuring cell viability of PANC1 cells after 48 h treatment with a dose course of gemcitabine. Two-way ANOVA, effect of CRISPR $^{***}P < 0.0001$, interaction of CRISPR and gemcitabine treatment $^{*}P = 0.0320$. $n = 3$ independent replicates, each condition performed in triplicate. (**E**) Western blot of cleaved caspase 3 and CYR61 (Santa Cruz) for PANC1 NTC and CYR61 CRISPR cells treated with a dose course of gemcitabine for 48 h. Two-way ANOVA, effect of CRISPR $^{*}P = 0.0108$. $n = 4$ independent replicates. (**F**) Cell Titer Glo assay measuring cell viability of MiaPaCa-2 cells after 48 h treatment with a dose course of gemcitabine. Two-way ANOVA, effect of CRISPR $^{***}P < 0.0001$, interaction of CRISPR and gemcitabine treatment $^{*}P = 0.0127$. $n = 3$ independent replicates, each condition performed in triplicate. (**G**) Western blot of cleaved caspase 3 and CYR61 (Santa Cruz) for MiaPaCa-2 NTC and CYR61 CRISPR cells treated with a dose course of gemcitabine for 48 h. Two-way ANOVA, effect of CRISPR $^{***}P < 0.0001$, Fisher's LSD, NTC versus CR1 $^{***}P < 0.0001$, NTC versus CR2 $P = 0.0965$. $n = 3$ independent replicates.

To examine whether CYR61 regulates gemcitabine-induced apoptosis in PDAC cells, we measured cell viability in response to a dose course of gemcitabine. CRISPR-mediated knockout of CYR61 significantly decreased cell viability in response to gemcitabine in PANC1 (Figure 2D) and MiaPaCa-2 cells (Figure 2F). Additionally, CRISPR-mediated knockout of CYR61 in PANC1 and MiaPaCa-2 cells resulted in increased levels of gemcitabine-induced apoptosis as shown by an increase in the levels of cleaved caspase 3 (Figure 2E and G). Knockout of CYR61 increased gemcitabine-induced Bax expression and decreased Bcl-2 expression in PANC1 cells (Supplementary Figure 3A, available at *Carcinogenesis* Online). In a reciprocal manner, adenovirus-mediated overexpression of CYR61 in CFPAC cells decreased gemcitabine-induced apoptosis (Supplementary Figure 3B, available at *Carcinogenesis* Online).

CYR61 expression is increased in PDAC

Bioinformatic analysis of a microarray dataset demonstrated that *CYR61* expression was increased in PDAC samples compared with matched normal adjacent tissue (Figure 3A and B), supporting increased CYR61 expression in PDAC, consistent with a prior report (32). Further analysis demonstrated that patients with familial PanIN precursor lesions (27) have an intermediate level of *CYR61* (Figure 3C). Although these assessments at the mRNA level were suggestive, serum protein levels of CYR61 in PDAC patients have not been investigated. Here we demonstrate that CYR61 protein expression is significantly elevated in the serum of PDAC patients, with a mean expression of 857.5 ng/ml compared with a mean expression of 508.5 ng/ml for healthy volunteers (Figure 3D). Further, survival data from the ICGC PACA-AU dataset demonstrated that PDAC patients with high levels of *CYR61* had a trend toward lower median survival time relative to patients with low *CYR61* expression (Figure 3E). Median survival time for the low *CYR61* group was 552 days, whereas median survival time for high *CYR61* group was 427 days.

CYR61 does not regulate expression of other gemcitabine resistance factors in PDAC

While nucleotide transporters are an important mechanism for regulating entry of gemcitabine into PDAC cells, there are several additional mechanisms that regulate resistance to gemcitabine in PDAC. Deoxycytidine kinase (dCK) phosphorylates gemcitabine to its active form once it enters the cytoplasm, and low expression of dCK is associated with worse survival after gemcitabine treatment (9,10). Additionally, high expression of the subunits of the enzyme ribonucleotide reductase (RRM1 and RRM2), which catalyzes the conversion of ribonucleotides to deoxynucleosides, is associated with gemcitabine resistance in patients (33–35). The expression of ATP-binding cassette transporters, which act as drug efflux pumps, is also associated with drug resistance in PDAC (36). The drug efflux pumps ABCB1 (MDR1/P-glycoprotein) and ABCC1 (MRP1) have been linked to the resistance of PDAC cells to gemcitabine (37,38). CYR61 has been previously reported to regulate expression of the drug efflux pump MDR1/P-glycoprotein in renal cell carcinoma (39), but it has not been studied in PDAC.

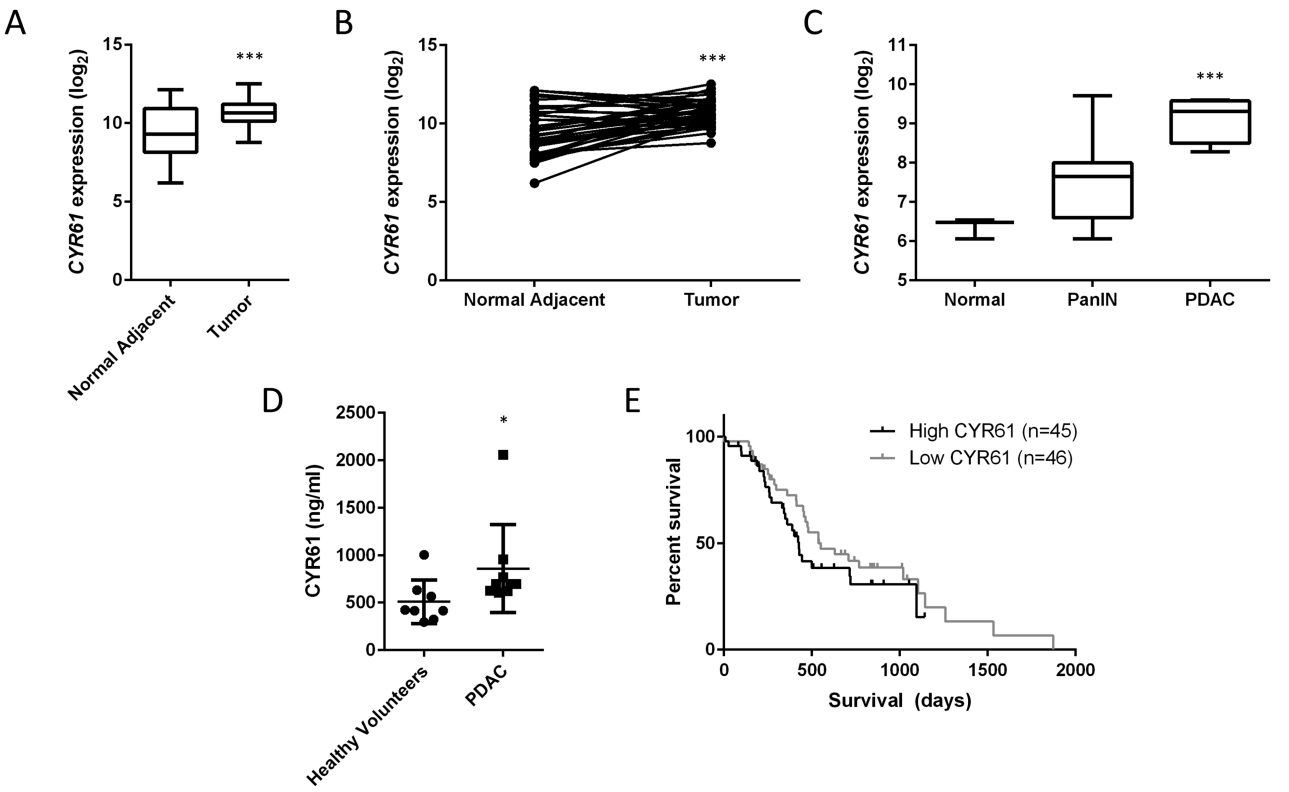

Figure 3. CYR61 expression is increased in tumor and serum patient samples in PDAC. (**A**) Microarray dataset analysis (GDS4103) for CYR61 expression in PDAC tumors. Mann–Whitney test, ***$P < 0.0001$. $n = 39$ patient samples. (**B**) Microarray dataset analysis (GDS4103) for CYR61 expression in PDAC tumors, comparing matched normal adjacent tissue with tumor tissue. Wilcoxon matched pairs signed rank test, ***$P < 0.0001$. Of 39 tumor samples, 29 had increased *CYR61* expression. (**C**) Microarray dataset analysis (GSE43288) for CYR61 expression in normal pancreas, familial PanIN lesions and PDAC tumors. Kruskal–Wallis test and Dunn's multiple comparison test, **$P = 0.0051$ for Normal versus PDAC. $n = 3$ for normal pancreas, $n = 13$ for PanIN, $n = 4$ for PDAC. (**D**) ELISA was performed on serum samples from healthy volunteers and PDAC patients. Mann–Whitney test, *$P = 0.0142$. $n = 8$ healthy volunteer samples, $n = 9$ PDAC samples. (**E**) Survival analysis of PDAC patients split by CYR61 expression from RNAseq analysis of the ICGC PACA-AU dataset. $P = 0.2389$.

We examined the effect of CYR61 on the expression of these factors associated with gemcitabine resistance. Either overexpression of CYR61 or CRISPR-mediated knockdown of CYR61 did not alter the expression levels of MDR1 or dCK at the protein level (Supplementary Figure 4A–C, available at *Carcinogenesis* Online). Additionally, there was no consistent or significant effect of CYR61 expression on the mRNA level of *RRM1*, *RRM2* or *ABCC1* (Supplementary Figure 4D–F, available at *Carcinogenesis* Online). Moreover, in PDAC patient samples, the level of *CYR61* did not significantly correlate with expression of these gemcitabine resistance factors (Supplementary Figure 5A–E, available at *Carcinogenesis* Online). These data suggest that CYR61 functions to mediate resistance to gemcitabine largely through its effects on the nucleotide transporters hENT1 and hCNT3.

Pancreatic stellate cells are a source of CYR61 in the PDAC tumor microenvironment

PDAC is characterized by an abundant fibrotic stroma that can comprise up to 80% of the tumor volume (40), making this stroma perhaps the most prominent of all epithelial cancers. This stroma contains PSCs, which are the predominant cells responsible for secretion of the extracellular matrix (ECM) components that comprise the fibrotic stroma (41–43). The microarray dataset used to examine *CYR61* expression analyzed whole-tissue tumor samples that include both cancer and stromal cells (26), suggesting that the PSCs might be a source of CYR61. To determine whether PSCs within the tumor microenvironment secrete CYR61, we examined RNAseq data that analyzed gene expression in PDAC tumors as well as three cell population isolated from the tumor: PSCs, tumor epithelial cells grown in patient-derived xenografts (PDXs) and tumor epithelial cells grown in *in vitro* cell culture (29). Isolated PSCs, identified as α-SMA positive, vimentin positive and EpCam negative (29), expressed significantly higher levels of *CYR61* compared with human tumor epithelial cells in patient-derived xenografts or *in vitro* cell culture (Figure 4A). PDAC samples expressed an intermediate amount, suggesting that the CYR61 from these samples is derived partly from stromal cells present in the samples. Isolated tumor

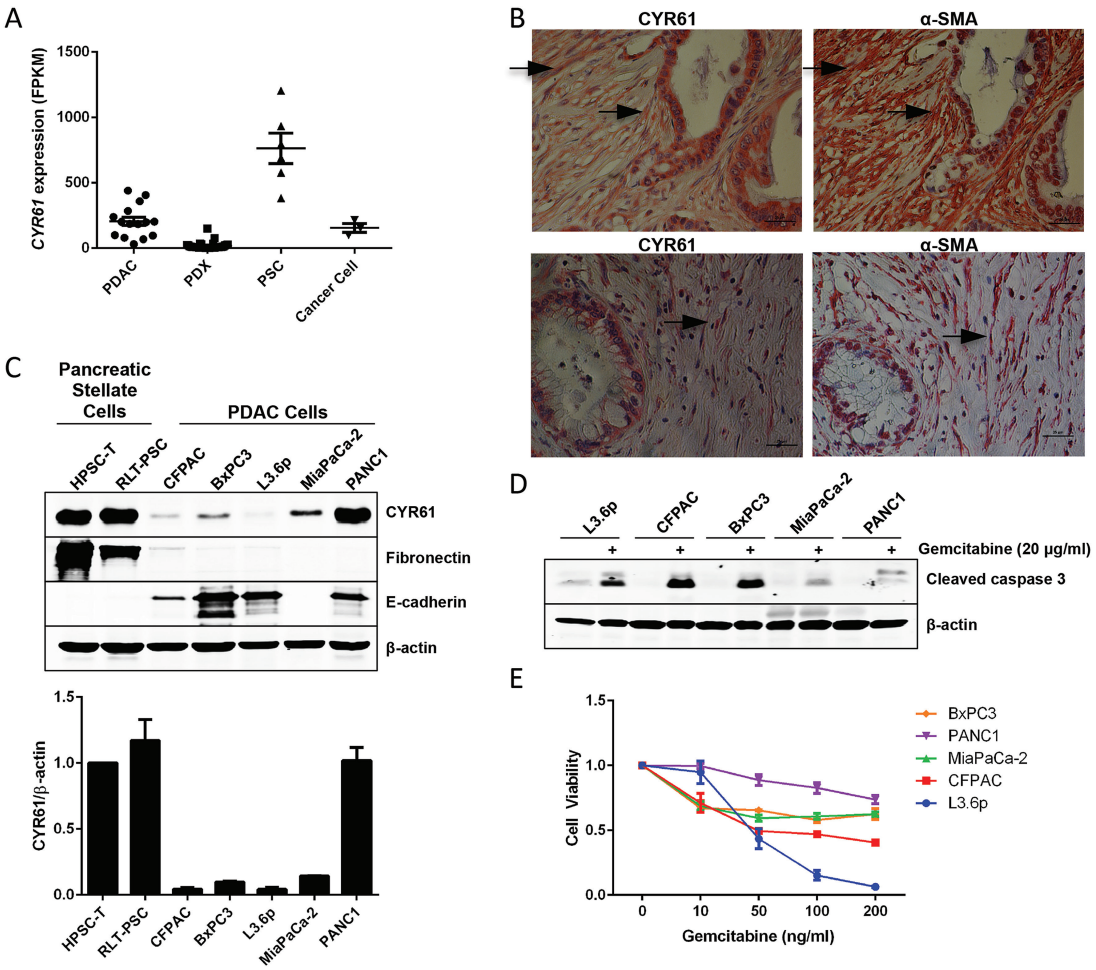

Figure 4. CYR61 is expressed by stromal PSCs in the tumor microenvironment. (**A**) *CYR61* expression from RNAseq data (29) in fragments per kilobase of transcript per million mapped reads in PDAC samples, PDXs, PSCs and isolated cancer cells cultured *in vitro* (cancer cell). PDX samples were processed with Xenome to sort human-specific epithelial expression from mouse-specific stromal expression (29). Kruskal–Wallis and Multiple Comparison Test, PDX versus PSCs. ***$P < 0.0001$, PDX versus PDAC. ***$P < 0.0001$. $n = 15$ for PDAC, $n = 37$ for PDX, $n = 6$ for PSCs, $n = 3$ for cancer cells. (**B**) IHC staining performed for CYR61 and α-SMA on human PDAC tissue using Warp Red Chromagen with hematoxylin counterstain. Arrows point to examples of cells positive for CYR61 and α-SMA. 40× magnification, scale bar is 25 μm (lower right). $n = 9$ PDAC samples, representative images shown for two samples. (**C**) Western blot of CYR61 (Santa Cruz) in immortalized human PSC cell lines (HPSC-T and RLT-PSC) and PDAC cell lines (CFPAC, BxPC3, L3.6p, MiaPaCa-2 and PANC1). Lysates were also probed for the mesenchymal marker fibronectin and the epithelial marker E-cadherin. $n = 3$ independent replicates. (**D**) Western blot of cleaved caspase 3 for PDAC cell lines treated with ±20 μg/ml gemcitabine for 48 h. Results are representative of three independent experiments. (**E**) Cell Titer Glo assay measuring cell viability of PDAC cell lines in response to a dose course of gemcitabine treatment for 48 h. $n = 3$ independent replicates, each condition performed in triplicate.

epithelial cells grown *in vitro* also had higher CYR61 expression than tumor cells grown in PDX (Figure 4A), suggesting that some PDAC epithelial cells may express higher levels of CYR61 in *in vitro* cell culture conditions as compensation for the lack of stromal-derived factors that are present *in vivo*.

To investigate expression of CYR61 at the protein level, we performed IHC staining for CYR61 on human PDAC tissue. PSCs in the tumor microenvironment were identified by staining for α-SMA on consecutive slides, and α-SMA staining in muscular arterial wall and duodenal smooth muscle (muscularis propria) overlying head of pancreas was used as a positive control (Supplementary Figure 6A, available at *Carcinogenesis* Online). IHC on human PDAC samples demonstrated co-localization of CYR61 staining with PSCs labeled by α-SMA (Figure 4B; Supplementary Figure 6, available at *Carcinogenesis* Online), indicating that PSCs are a source of CYR61 in the tumor microenvironment. Consistent with a previous report (32), most PDAC epithelial cells also stained positive for CYR61 (Figure 4B; Supplementary Figure 6, available at *Carcinogenesis* Online), although some PDAC epithelial cells showed weak CYR61 staining (Supplementary Figure 6D and E, available at *Carcinogenesis* Online). α-SMA negative fibroblasts near acinar cells did not stain positive for CYR61 (Supplementary Figure 6H and I, available at *Carcinogenesis* Online).

In addition, we evaluated expression of CYR61 in five PDAC cell lines and two human PSC cell lines, HPSC-T (18) and RLT-PSC (17), which were isolated from PDAC and chronic pancreatitis samples, respectively. We validated the identity of PSCs by confirming expression of the PSC-specific markers α-SMA, vimentin, collagen 1α1 and desmin (Supplementary Figure 7, available at *Carcinogenesis* Online). The mesenchymal PSCs expressed high levels of the ECM protein fibronectin, whereas most PDAC cells expressed higher levels of the epithelial marker E-cadherin (Figure 4C). The PSC cell lines had higher CYR61 expression than the majority of PDAC cell lines (Figure 4C). Interestingly, the PANC1 cell line also had high expression of CYR61 (Figure 4C). Consistent with a role for CYR61 in gemcitabine resistance, pancreatic cancer cell lines that express higher levels of CYR61 were more resistant to gemcitabine-induced apoptosis *in vitro* (Figure 4D and E).

TGF-β signaling induces CYR61 expression in PSCs in the PDAC tumor microenvironment

CYR61 has been demonstrated to be regulated by both the transforming growth factor-β (TGF-β) signaling and Hippo-YAP/TAZ signaling pathways (44,45). TGF-β ligand expression is elevated in PDAC, and patients with high levels of TGF-β1 ligand in their serum have a significantly worse prognosis (46). However, mutations that inactive the canonical TGF-β-Smad signaling pathway are common in PDAC, with around 55% of PDAC patients having inactivating mutations in *SMAD4* (47). Therefore, elevated TGF-β may negatively affect PDAC progression or therapy response in part through stromal cells with intact *SMAD4*, including PSCs. Consistent with this hypothesis, in the microarray dataset that analyzed gene expression in whole-tissue PDAC samples, *CYR61* expression significantly correlated with expression of the *TGFB1* ligand and also with the well-established TGF-β target genes *SERPINE1* (PAI-1) and *SMAD7* (Figure 5A–C). Moreover, in the rat PSC cell line LTC-14 (19) and the mouse PSC cell line imPSC (20), which were isolated from normal pancreas and have low basal CYR61 expression, TGF-β induced CYR61 expression in a dose-dependent fashion (Figure 5D). TGF-β induced CYR61 protein expression as early as 6 h post treatment and mRNA expression as early as 3 h post treatment, suggesting that the induction of CYR61 by TGF-β was a direct effect and not via induction of other growth factors (Figure 5E and F).

TGF-β induces activation of canonical Smad signaling in PSCs, but TGF-β also induces activation of several noncanonical signaling pathways, including p38 MAPK and PI3K-Akt signaling (Figure 5G; Supplementary Figure 8A, available at *Carcinogenesis* Online). To determine which downstream signaling pathways were important for TGF-β-induced CYR61 expression in PSCs, we pretreated PSCs with kinase inhibitors against ALK5, p38 MAPK and PI3K and examined the effect on TGF-β-induced CYR61 expression. Treatment with the ALK5 inhibitor, but not the p38 MAPK or PI3K-Akt inhibitor, blocked TGF-β-induced CYR61 expression (Figure 5H; Supplementary Figure 8B, available at *Carcinogenesis* Online). We confirmed that these inhibitors blocked activation of downstream targets in the LTC-14 PSCs (Supplementary Figure 8C–E, available at *Carcinogenesis* Online). Further, CRISPR-mediated knockdown of Smad2 and Smad3 in the LTC-14 PCSs decreased TGF-β-induced CYR61 expression (Figure 5I), with the level of knockdown of both Smads correlating with the loss of TGF-β induction. In addition, expression of CA-ALK5 induced CYR61 expression in LTC-14 and imPSC cells (Supplementary Figure 8F and G, available at *Carcinogenesis* Online). These results suggest that TGF-β induces CYR61 expression in PSCs through canonical TGF-β-ALK5-Smad signaling.

TGF-β did not induce CYR61 in Smad4-null cells (CFPAC and BxPC3) or TGF-β nonresponsive MiaPaCa-2 cells (48) (Supplementary Figure 9A and B, available at *Carcinogenesis* Online). Human PSC cell lines HPSC-T and RLT-PSC had high basal CYR61 expression (Figure 4C), likely because they were isolated from PDAC and chronic pancreatitis samples. However, ELISA data demonstrate that activation of TGF-β signaling by expression of a constitutively active version of the TGF-β receptor ALK5 (CA-ALK5) induced even higher secretion of CYR61 (Supplementary Figure 9B). Although *CYR61* expression significantly correlated with expression of the Hippo target gene *AXL* in PDAC samples (Supplementary Figure 10A, available at *Carcinogenesis* Online), activation of Hippo signaling in LTC-14 PSCs through expression of constitutively active YAP (YAP5SA) only moderately induced CYR61 expression relative to TGF-β treatment (Supplementary Figure 10B, available at *Carcinogenesis* Online).

TGF-β-Induced CYR61 promotes gemcitabine resistance in an *in vitro* co-culture assay

To examine the role of TGF-β-induced CYR61 in PSCs on gemcitabine-induced apoptosis of cancer cells, we established an *in vivo* co-culture assay where PDAC cells were treated with CM from PSCs with activated TGF-β signaling (Figure 6A). To examine the role of stromal CYR61, LTC-14 PSCs were infected with adenoviruses to express CYR61 or CA-ALK5 with a luciferase adenovirus used as a control (Figure 6B). We verified that activation of TGF-β signaling in LTC-14 PSCs through expression of CA-ALK5 releases soluble CYR61 into the CM (Figure 6C). CM from PSCs with CYR61 expression or CA-ALK5 protected CFPAC cells from gemcitabine-induced apoptosis as shown by reduced levels of cleaved caspase 3 (Figure 6D). Similar results were obtained in the BxPC3 cell line (Supplementary Figure 10C). In contrast, expression of constitutively active YAP in LTC-14 PSCs only weakly induced CYR61 and did not affect the gemcitabine-induced apoptosis of PDAC cells in our *in vitro* co-culture model (Supplementary Figure 10D, available at *Carcinogenesis* Online), suggesting that TGF-β signaling was the primary pathway inducing CYR61 expression in PSCs. Finally, *in silico* analysis of whole-tissue PDAC samples demonstrated that *TGFB1* ligand

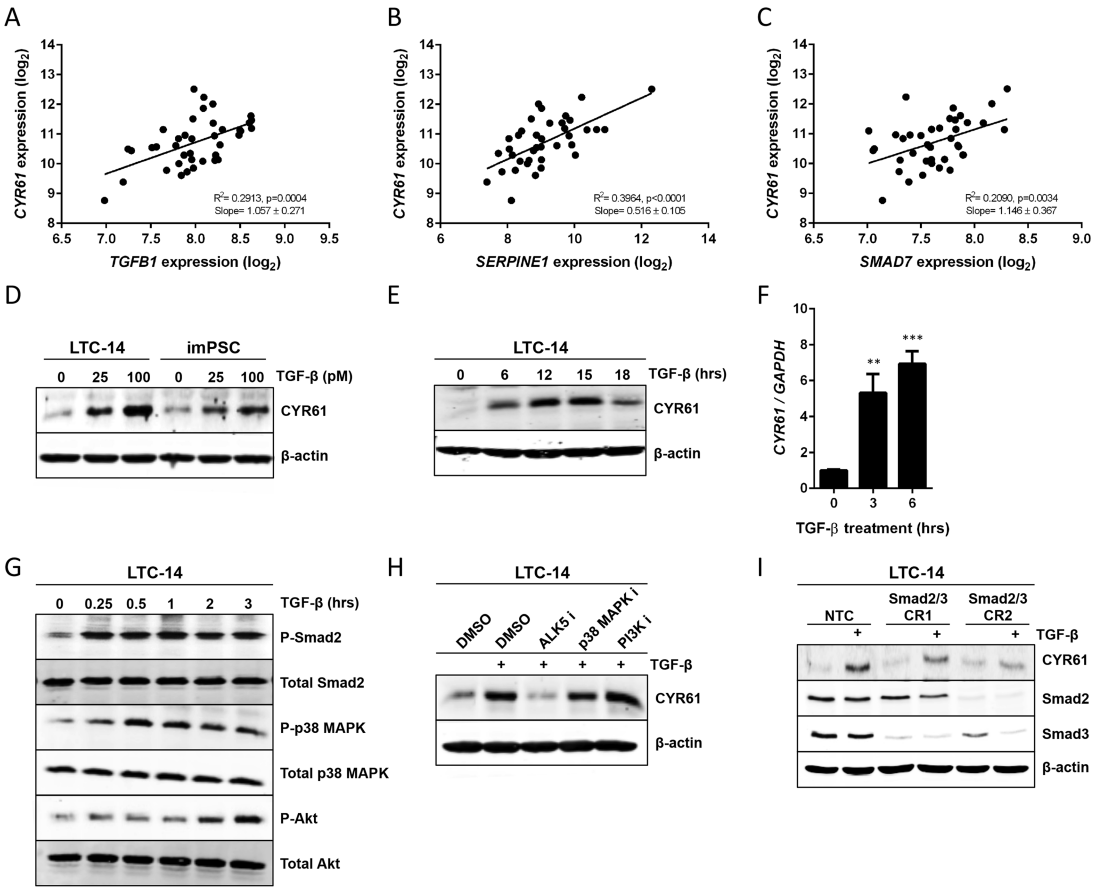

Figure 5. TGF-β-ALK5-Smad signaling induces CYR61 expression in pancreatic stellate cells. (**A–C**) Linear regression was performed using the microarray dataset GDS4103. *n* = 39 patient samples: (**A**) *TGFB1*, (**B**) *SERPINE1* and (**C**) *SMAD7*. (**D**) Western blot of CYR61 (Abcam) in LTC-14 and imPSC cells that were serum starved in 1% FBS then treated with indicated doses of TGF-β1 for 16 h. (**E**) Western blot of CYR61 (Abcam) in LTC-14 cells that were serum starved in 1% FBS then treated with 100 pM TGF-β for indicated times. (**F**) Quantitative RT-PCR for *rCYR61* performed on LTC-14 cells treated with 100 pM TGF-β for 0, 3 or 6 h. ANOVA ***P = 0.0002, Dunnett's multiple comparison test, 0 h versus 3 h **P = 0.003, 0 h versus 6 h ***P = 0.0001. *n* = 3 replicates. (**G**) Western blot analyzing downstream TGF-β signaling. LTC-14 cells were serum starved in 1% FBS then treated with 100 pM TGF-β1 ligand for indicated times. (**H**) Western blot of CYR61 (Abcam) in LTC-14 cells pretreated with DMSO vehicle control or inhibitors against ALK5 (20 μM SB431542), p38 MAPK (10 μM SB203580) or PI3K (10 μM LY294002) for 30 min then treated with 100 pM TGF-β1 for 16 h. (**I**) Western blot for CYR61 (Abcam), Smad2 and Smad3 in LTC-14 cells stably expressing NTC or CRISPR constructs against both Smad2 and Smad3. All western blotting results are representative of three independent experiments.

expression negatively correlates with expression of *SLC29A1* (*hENT1*) and *SLC28A3* (*hCNT3*) (Figure 6E and F), suggesting that TGF-β plays a role in regulating these nucleoside transporters *in vivo*.

Discussion

Chemotherapy resistance is a major clinical problem in PDAC. Even one of the commonly used first-line agents, gemcitabine, has a very low response rate and only modestly prolongs survival. Therefore, it is important to understand the cellular mechanisms that regulate resistance to gemcitabine. Our results demonstrate that CYR61 promotes resistance to gemcitabine predominantly by modulating the levels of the nucleoside transporters that mediate cellular uptake of gemcitabine. The role of the stroma in therapy resistance is an emerging area of interest in PDAC with recent genetic mouse models and clinical trials that target PSCs having conflicting results, with both positive and negative effects on cancer progression and response to gemcitabine (49–52). Understanding what aspects of PSCs promote therapy resistance and identifying signaling mechanisms that regulate this are important to effectively target the stroma. Here we demonstrate that stromal-derived CYR61 has an important role in promoting gemcitabine resistance through downregulation of the nucleoside transporters hENT1 and hCNT3.

We have demonstrated that TGF-β strongly induces CYR61 expression in PSCs. A recent phase II clinical trial suggested that addition of the TGF-β inhibitor galsunisertib to gemcitabine led to improved overall and progression-free survival in PDAC patients compared with gemcitabine alone (53). Due to the pleotropic homeostatic functions of TGF-β, global inhibition of TGF-β signaling does have the potential to have side effects. Therefore, understanding the specific downstream effectors of TGF-β signaling in PDAC is important for development of future therapies. Our results indicate that stromal TGF-β signaling promotes resistance to gemcitabine in PDAC cells via induction of CYR61. TGF-β is a major driver of EMT (54), and EMT has recently been shown to regulate gemcitabine resistance and expression of hENT1 and hCNT3 in PDAC (14). Whether additional TGF-β-induced genes promote gemcitabine resistance through regulation of these nucleoside transporters, and whether CYR61 mediates the effects of TGF-β on EMT in PDAC (32), remains to be established.

CYR61 is a member of the CCN family of matricellular proteins, which includes CTGF and NOV. Targeting the CCN family member CTGF in combination with gemcitabine in PDAC

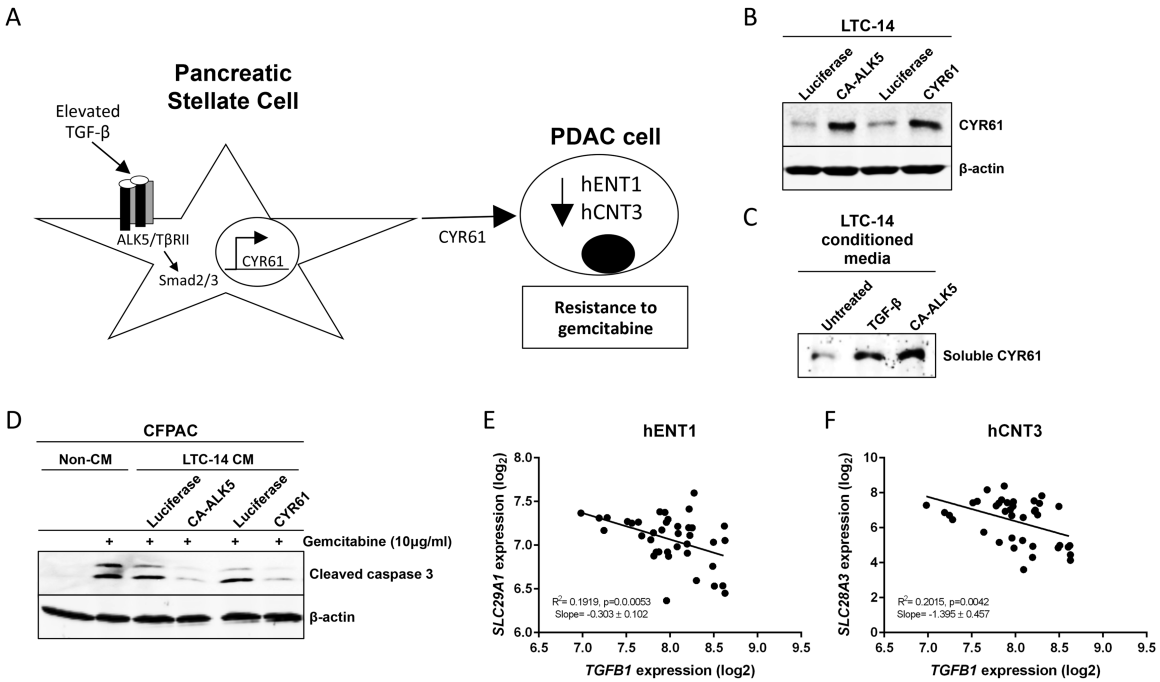

Figure 6. Expression of CYR61 and activation of TGF-β signaling in PSCs promote resistance to gemcitabine-induced apoptosis in an *in vitro* co-culture assay. (**A**) Model of *in vitro* co-culture assay examining the effect of TGFβ-induced CYR61 derived from PSCs on gemcitabine-induced apoptosis of PDAC cells. (**B**) Western blot of CYR61 (Abcam) in LTC-14 cells. LTC-14 cells were infected with CA-ALK5 or luciferase control adenovirus or CYR61 or luciferase control adenovirus at an MOI of 100 for 48 h. (**C**) Western blot of CYR61 (Abcam) in LTC-14 condensed CM following treatment with 100 pM TGF-β1 or infected with CA-ALK5 adenovirus at an MOI of 25 for 48 h. (**D**) Western blot of cleaved caspase 3 in CFPAC cells treated with 10 μg/ml gemcitabine for 48 h. CFPAC cells were pretreated for 24 h with CM collected from LTC-14 cells or nonconditioned media (non-CM) as a control. CM was collected from LTC-14 cells infected with adenoviruses as indicated in panel B. (**E**, **F**) Linear regression using the microarray dataset GDS4103. $n = 39$ patient samples: (**E**) *hENT1* (*SLC29A1*) and (**F**) *hCNT3* (*SLC28A3*). All western blotting results are representative of three independent experiments.

has shown promise in a preclinical mouse model (55), and the CTGF neutralizing antibody FG-3019 is being tested in an ongoing clinical trial (56). However, although CTGF and CYR61 are structurally similar, the FG-3019 neutralizing antibody does not interact with CYR61 (57). The current results regarding the role of CYR61 in gemcitabine resistance provide a rationale for inhibiting CYR61 or both CTGF and CYR61 in combination with gemcitabine (and nab-paclitaxel) in PDAC patients. Although our study is the first to identify a role for CYR61 in nucleoside transporter expression and gemcitabine resistance, CYR61 has recently been implicated in therapy resistance in the contexts of several other cancers, including renal cell carcinoma (39), breast cancer (58,59), acute myeloid leukemia (60) and ovarian cancer (61), which indicates that CYR61 may be a promising target to improve efficacy of chemotherapy.

In summary, here we have identified that the matricellular protein CYR61 is induced by the TGF-β-ALK5-Smad signaling pathway in PSCs in the tumor microenvironment, where it negatively regulates the expression of the nucleoside transporters hENT1 and hCNT3 in PDAC to mediate resistance to gemcitabine.

Supplementary material

Supplementary Figures S1–S10 and Tables S1–S4 can be found at http://carcin.oxfordjournals.org/

Funding

National Institutes of Health (F31-CA180602 to R.A.H., F30-CA196162 to J.J.H., R01-CA135006 to G.C.B., R01-CA136786 to G.C.B. and R21-CA198287 to R.R.W.).

Acknowledgements

The authors thank Tam How for assistance with adenovirus preparation, Angela Gaviglio for help with microarray dataset analysis and Melissa Hector-Greene for assistance with development of CRISPR/Cas9 constructs.
Conflict of Interest Statement: None declared.

References

1. Siegel, R. et al. (2014) Cancer statistics, 2014. CA: A Cancer J. Clin., 64, 9–29.
2. Rahib, L. et al. (2014) Projecting cancer incidence and deaths to 2030: the unexpected burden of thyroid, liver, and pancreas cancers in the United States. Cancer Res., 74, 2913–2921.
3. de Sousa Cavalcante, L. et al. (2014) Gemcitabine: metabolism and molecular mechanisms of action, sensitivity and chemoresistance in pancreatic cancer. Eur. J. Pharmacol., 741, 8–16.
4. Burris, H.A. 3rd et al. (1997) Improvements in survival and clinical benefit with gemcitabine as first-line therapy for patients with advanced pancreas cancer: a randomized trial. J. Clin. Oncol., 15, 2403–2413.
5. Garrido-Laguna, I. et al. (2015) Pancreatic cancer: from state-of-the-art treatments to promising novel therapies. Nat. Rev. Clin. Oncol., 12, 319–334.
6. Gray, J.H. et al. (2004) The concentrative nucleoside transporter family, SLC28. Pflugers. Arch., 447, 728–734.
7. Baldwin, S.A. et al. (2004) The equilibrative nucleoside transporter family, SLC29. Pflugers. Arch., 447, 735–743.
8. Paproski, R.J. et al. (2013) Human concentrative nucleoside transporter 3 transfection with ultrasound and microbubbles in nucleoside transport deficient HEK293 cells greatly increases gemcitabine uptake. PLoS One, 8, e56423.
9. Fujita, H. et al. (2010) Gene expression levels as predictive markers of outcome in pancreatic cancer after gemcitabine-based adjuvant chemotherapy. Neoplasia, 12, 807–817.

10. Maréchal, R. et al. (2012) Levels of gemcitabine transport and metabolism proteins predict survival times of patients treated with gemcitabine for pancreatic adenocarcinoma. Gastroenterology, 143, 664–674.e1.
11. Liu, Z.Q. et al. (2014) Prognostic value of human equilibrative nucleoside transporter1 in pancreatic cancer receiving gemcitabin-based chemotherapy: a meta-analysis. PLoS One, 9, e87103.
12. Maréchal, R. et al. (2009) Human equilibrative nucleoside transporter 1 and human concentrative nucleoside transporter 3 predict survival after adjuvant gemcitabine therapy in resected pancreatic adenocarcinoma. Clin. Cancer Res., 15, 2913–2919.
13. Elnaggar, M. et al. (2012) Molecular targets of gemcitabine action: rationale for development of novel drugs and drug combinations. Curr. Pharm. Des., 18, 2811–2829.
14. Zheng, X. et al. (2015) Epithelial-to-mesenchymal transition is dispensable for metastasis but induces chemoresistance in pancreatic cancer. Nature, 527, 525–530.
15. Skrypek, N. et al. (2015) The oncogenic receptor ErbB2 modulates gemcitabine and irinotecan/SN-38 chemoresistance of human pancreatic cancer cells via hCNT1 transporter and multidrug-resistance associated protein MRP-2. Oncotarget, 6, 10853–10867.
16. Bruns, C.J. et al. (1999) *In vivo* selection and characterization of metastatic variants from human pancreatic adenocarcinoma by using orthotopic implantation in nude mice. Neoplasia, 1, 50–62.
17. Jesnowski, R. et al. (2005) Immortalization of pancreatic stellate cells as an *in vitro* model of pancreatic fibrosis: deactivation is induced by matrigel and N-acetylcysteine. Lab. Invest., 85, 1276–1291.
18. Hwang, R.F. et al. (2008) Cancer-associated stromal fibroblasts promote pancreatic tumor progression. Cancer Res., 68, 918–926.
19. Sparmann, G. et al. (2004) Generation and characterization of immortalized rat pancreatic stellate cells. Am. J. Physiol. Gastrointest. Liver Physiol., 287, G211–G219.
20. Mathison, A. et al. (2010) Pancreatic stellate cell models for transcriptional studies of desmoplasia-associated genes. Pancreatology, 10, 505–516.
21. Ueda, Y. et al. (2004) Overexpression of HER2 (erbB2) in human breast epithelial cells unmasks transforming growth factor beta-induced cell motility. J. Biol. Chem., 279, 24505–24513.
22. Liu, H. et al. (2008) Cysteine-rich protein 61 and connective tissue growth factor induce deadhesion and anoikis of retinal pericytes. Endocrinology, 149, 1666–1677.
23. Hasan, A. et al. (2011) The matricellular protein cysteine-rich protein 61 (CCN1/Cyr61) enhances physiological adaptation of retinal vessels and reduces pathological neovascularization associated with ischemic retinopathy. J. Biol. Chem., 286, 9542–9554.
24. Sanjana, N.E. et al. (2014) Improved vectors and genome-wide libraries for CRISPR screening. Nat. Methods, 11, 783–784.
25. Shalem, O. et al. (2014) Genome-scale CRISPR-Cas9 knockout screening in human cells. Science, 343, 84–87.
26. Badea, L. et al. (2008) Combined gene expression analysis of whole-tissue and microdissected pancreatic ductal adenocarcinoma identifies genes specifically overexpressed in tumor epithelia. Hepatogastroenterology, 55, 2016–2027.
27. Crnogorac-Jurcevic, T. et al. (2013) Molecular analysis of precursor lesions in familial pancreatic cancer. PLoS One, 8, e54830.
28. Scarlett, C.J. et al. (2011) Precursor lesions in pancreatic cancer: morphological and molecular pathology. Pathology, 43, 183–200.
29. Moffitt, R.A. et al. (2015) Virtual microdissection identifies distinct tumor- and stroma-specific subtypes of pancreatic ductal adenocarcinoma. Nat. Genet., 47, 1168–1178.
30. Mackey, J.R. et al. (1998) Functional nucleoside transporters are required for gemcitabine influx and manifestation of toxicity in cancer cell lines. Cancer Res., 58, 4349–4357.
31. Leask, A. et al. (2006) All in the CCN family: essential matricellular signaling modulators emerge from the bunker. J. Cell Sci., 119, 4803–4810.
32. Haque, I. et al. (2011) Cyr61/CCN1 signaling is critical for epithelial-mesenchymal transition and stemness and promotes pancreatic carcinogenesis. Mol. Cancer, 10, 8.
33. Duxbury, M.S. et al. (2004) RNA interference targeting the M2 subunit of ribonucleotide reductase enhances pancreatic adenocarcinoma chemosensitivity to gemcitabine. Oncogene, 23, 1539–1548.
34. Xie, H. et al. (2013) Predictive and prognostic roles of ribonucleotide reductase M1 in resectable pancreatic adenocarcinoma. Cancer, 119, 173–181.
35. Nakahira, S. et al. (2007) Involvement of ribonucleotide reductase M1 subunit overexpression in gemcitabine resistance of human pancreatic cancer. Int. J. Cancer, 120, 1355–1363.
36. König, J. et al. (2005) Expression and localization of human multidrug resistance protein (ABCC) family members in pancreatic carcinoma. Int. J. Cancer, 115, 359–367.
37. Nath, S. et al. (2013) MUC1 induces drug resistance in pancreatic cancer cells via upregulation of multidrug resistance genes. Oncogenesis, 2, e51.
38. Zhang, W. et al. (2013) Emodin sensitizes the gemcitabine-resistant cell line Bxpc-3/Gem to gemcitabine via downregulation of NF-κB and its regulated targets. Int. J. Oncol., 42, 1189–1196.
39. Long Q.Z. et al. (2013) Interaction of CCN1 with alphavbeta3 integrin induces P-glycoprotein and confers vinblastine resistance in renal cell carcinoma cells. Anticancer Drugs, 24, 810–817.
40. Erkan M. et al. (2012) The impact of the activated stroma on pancreatic ductal adenocarcinoma biology and therapy resistance. Curr. Mol. Med., 12, 288–303.
41. Bachem, M.G. et al. (2005) Pancreatic carcinoma cells induce fibrosis by stimulating proliferation and matrix synthesis of stellate cells. Gastroenterology, 128, 907–921.
42. Yen, T.W. et al. (2002) Myofibroblasts are responsible for the desmoplastic reaction surrounding human pancreatic carcinomas. Surgery, 131, 129–134.
43. Apte, M.V. et al. (2004) Desmoplastic reaction in pancreatic cancer: role of pancreatic stellate cells. Pancreas, 29, 179–187.
44. Jun, J.I. et al. (2011) Taking aim at the extracellular matrix: CCN proteins as emerging therapeutic targets. Nat. Rev. Drug Discov., 10, 945–963.
45. Bartholin, L. et al. (2007) The human Cyr61 gene is a transcriptional target of transforming growth factor beta in cancer cells. Cancer Lett., 246, 230–236.
46. Javle, M. et al. (2014) Biomarkers of TGF-β signaling pathway and prognosis of pancreatic cancer. PLoS One, 9, e85942.
47. Hahn, S.A. et al. (1996) DPC4, a candidate tumor suppressor gene at human chromosome 18q21.1. Science, 271, 350–353.
48. Simeone, D.M. et al. (2000) Disruption of TGFbeta signaling pathways in human pancreatic cancer cells. Ann. Surg., 232, 73–80.
49. Rhim, A.D. et al. (2014) Stromal elements act to restrain, rather than support, pancreatic ductal adenocarcinoma. Cancer Cell, 25, 735–747.
50. Sherman, M.H. et al. (2014) Vitamin D receptor-mediated stromal reprogramming suppresses pancreatitis and enhances pancreatic cancer therapy. Cell, 159, 80–93.
51. Özdemir, B.C. et al. (2014) Depletion of carcinoma-associated fibroblasts and fibrosis induces immunosuppression and accelerates pancreas cancer with reduced survival. Cancer Cell, 25, 719–734.
52. Provenzano, P.P. et al. (2012) Enzymatic targeting of the stroma ablates physical barriers to treatment of pancreatic ductal adenocarcinoma. Cancer Cell, 21, 418–429.
53. Melisi, D. et al. (2016) A phase II, double-blind study of galunisertib+gemcitabine (GG) vs gemcitabine+placebo (GP) in patients (pts) with unresectable pancreatic cancer (PC). 2016 ASCO Annual Meeting. J Clin Oncol, 34, abstract 4019.
54. Lamouille, S. et al. (2014) Molecular mechanisms of epithelial-mesenchymal transition. Nat. Rev. Mol. Cell Biol., 15, 178–196.
55. Neesse, A. et al. (2013) CTGF antagonism with mAb FG-3019 enhances chemotherapy response without increasing drug delivery in murine ductal pancreas cancer. Proc. Natl. Acad. Sci. USA, 110, 12325–12330.
56. Dimou, A. et al. (2013) Novel agents in the treatment of pancreatic adenocarcinoma. J. Pancreas, 14, 138–140.
57. Wang, Q. et al. (2011) Cooperative interaction of CTGF and TGF-β in animal models of fibrotic disease. Fibrogenesis Tissue Repair, 4, 4.
58. Lin, M.T. et al. (2004) Cyr61 expression confers resistance to apoptosis in breast cancer MCF-7 cells by a mechanism of NF-kappaB-dependent XIAP up-regulation. J. Biol. Chem., 279, 24015–24023.
59. Menendez, J.A. et al. (2005) A novel CYR61-triggered 'CYR61-alphavbeta3 integrin loop' regulates breast cancer cell survival and chemosensitivity through activation of ERK1/ERK2 MAPK signaling pathway. Oncogene, 24, 761–779.
60. Long, X. et al. (2015) Stromal CYR61 confers resistance to mitoxantrone via spleen tyrosine kinase activation in human acute myeloid leukaemia. Br. J. Haematol., 170, 704–718.
61. Lee, K.B. et al. (2012) CYR61 controls p53 and NF-κB expression through PI3K/Akt/mTOR pathways in carboplatin-induced ovarian cancer cells. Cancer Lett., 315, 86–95.